STRAIN SOFTENING ANALYSIS FOR IDENTIFICATION AND PREDICTION OF DEFORMATIONAL BEHAVIOR OF A SHALLOW NATM TUNNEL

Jaeho LEE[1], Shinichi AKUTAGAWA[2], Takashi KITAGAWA[3], Atsumi ISOGAI[4] and Takeshi MATSUNAGA[5]

[1]Member of JSCE, Graduate student, Kobe University
(Rokkodai 1-1, Nada, Kobe, 657-8501, Japan)
E-mail : 006d804n@y02.kobe-u.ac.jp
[2]Member of JSCE, Associate Professor, Dept. of Architecture and Civil Engineering, Kobe University
(Rokkodai 1-1, Nada-ku, Kobe, 657-8501, Japan)
E-mail : cadax@kobe-u.ac.jp
[3]Member of JSCE, Japan Railway Construction, Transport and Technology Agency, Tokyo, Japan
(Gioncyou 2-1, Hakata-ku, Fukuoka, 812-8622, Japan)
E-mail : tak.kitagawa@jrtt.go.jp
[4]Member of JSCE, Japan Railway Construction, Transport and Technology Agency, Tokyo, Japan
(Honmachi 6-50-1, Naka-ku, Yokohama, 231-8315, Japan)
E-mail : a.isogai@jrtt.go.jp
[5]Member of JSCE, Pacific Consultants CO., LTD., Tokyo, Japan
(Nishi Shinjuku 2-7-1, Shinjuku-ku, 163-0730, Tokyo)
E-mail : takeshi.matsunaga@tk.pacific.co.jp

A finite element analysis procedure considering strain softening behavior is applied for identification and prediction of deformational behavior around a shallow NATM tunnel. The proposed approach produced a strain distribution, deformational mechanism and surface settlement profile, which are in good agreement with the results of the field measurement conducted at two cross sections with different deformational characteristics. The predictive capability of the method was also tested at three different stages in which higher accuracy of prediction was achieved accordingly in latter stages.

Key Words : *NATM tunnel, strain softening analysis, shear band, prediction*

1. INTRODUCTION

Currently an increasing number of urban tunnels with small overburden are excavated according to the principle of the New Austrian Tunneling Method (NATM). In urban area, constructions of soft ground tunnels are usually important in terms of prediction and control of surface settlement and gradient[1)]. Several approaches[2)-5)] are readily used for prediction of the ground deformations associated with tunneling. In recent years, numerical methods for design purposes are often used to predict deformational behavior around tunnels. Finite element procedures have been applied not only to the ground movement prediction but also to the whole tunnel design problem, which includes simulation of the construction method, analysis of the extent and development of failed zones, design of the support system, and effects on nearby tunnels, etc. In the approach of numerical modeling, those results are strongly dependent on the construction stages modeled, the constitutive law selected, and the appropriate assessment of the corresponding soil parameters. However, it is still difficult under the present state of the art to predict deterministically the behavior of the ground and tunnel system in the planning and design state, thereby resulting in an extensive difference between the predicted values and the actual behavior after excavation. In this paper, finite element simulation has been applied to predict ground movement caused by tunneling of a shallow NATM tunnel in unconsolidated soil. The method used here incorporates reduction of shear stiffness, as well as strain softening effects of given material strength parameters[4]. Numerical simulation, firstly, is performed with material property values, E, ν, c, and ϕ, obtained from laboratory. Secondly, a series of parameter tuning is performed for better agreement between computed and measured quantities at arrival and finish of the top heading excavation. The parameters identified at these stages were then used to predict displacements at the final stage. Potential minimum and maximum displacements thus obtained forming a banded prediction, showed that the actual displacement measured would fall in this predicted band of displacement. Thus, it is stressed in this paper that the proper consideration of nonlinear nature of ground materials is necessary not only for identification of deformational mechanism which has already happened, but also for predicting what to expect with reasonably high accuracy.

2. PREDICTION VERSUS REALITY

Fig.1 is a typical illustration of displacement; say surface settlement, observed during staged tunnel construction process. While construction is in early stage, it is often observed that deformational mechanism around the tunnel is still in an elastic state, therefore, predicted displacement easily agrees with actual one measured.

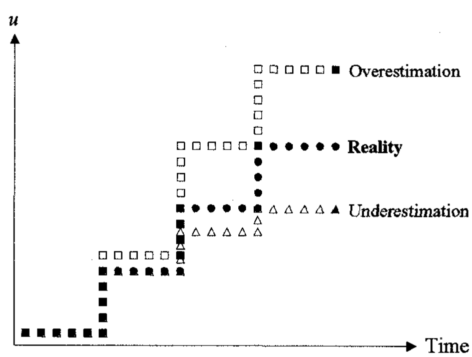

Fig.1 Displacement versus time.

However, as construction progresses, nonlinear nature of stress-strain relationship starts to play a role, making the whole deformational process far more complex than before. This is the most likely reason that predicted behavior of tunnel deformation at final stage could easily underestimate or overestimate the reality, sometimes with a large margin.

Fig.2 shows measured displacements (surface subsidence and crown settlements) plotted against predicted ones for several tunnels with shallow overburden. It is recognized that in most cases the measured ones are smaller than the predicted values in design stages. This is an indication that design parameters are chosen in such a way that safety and stability of tunnels during construction be assured.

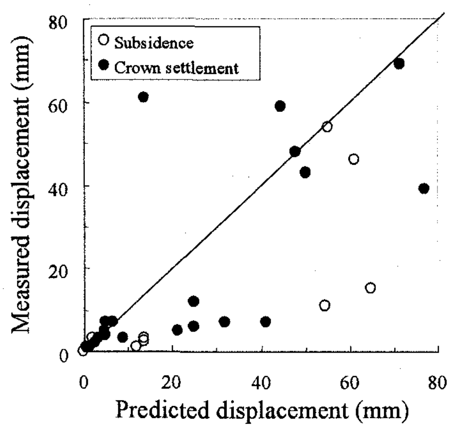

Fig.2 Measured versus predicted displacements.

The assurance of safety and control of displacement during construction is off course one of the most important issues. However, in some cases, the tunnel design could be overly safe when uncertainties arise in setting up key parameters used in design, largely due to a complicated nonlinear deformational mechanism identified around shallow tunnels. One notices, therefore, that not only accuracy of final state of tunnel deformation, but also accuracy of prediction throughout the process of tunnel construction, is to be improved such that overall management of tunnel safety during construction is guaranteed at high level.

3. NONLINEAR DEFORMATION IN SHALLOW TUNNELS

Deformational behavior around a shallow tunnel is often characterized by formation of shear bands developing from tunnel shoulder reaching, sometimes, to the ground surface. **Fig.3** shows a strain distribution derived from the results of displacement measurements taken from a subway tunnel in Washington D.C.[6]

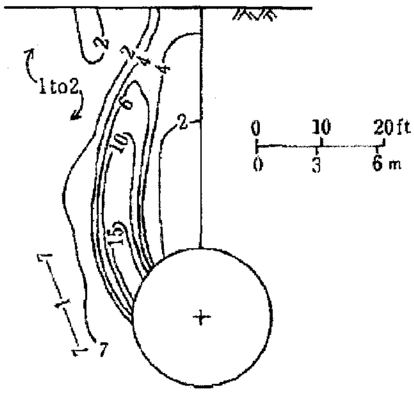

Fig.3 Strain distribution around a subway tunnel (after Hansmire and Cording, 1985[6]).

One possible explanation of this deformational behavior may be best stated with a help of an illustration given in **Fig.4**. Region-A, surrounded by slip plane *k-k*, is regarded as a potentially unstable zone that may displace downward at the lack of frictional support along *k-k* planes. What is separating region-A from the surrounding is shear band ***a*** formed along *k-k* line with some thickness, as region A slides downward. The adjacent region-B follows the movement of region-A, leading to the formation of another shear band ***b***. The direction of shear band ***b*** is related to $45^\circ + \phi/2$ (ϕ: friction angle) and often coincides with what is called a boundary line of zone influenced by excavation.

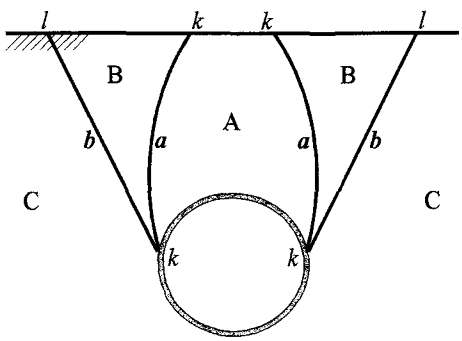

Fig.4 Typical deformational mechanism around a shallow tunnel.

Regions A and B correspond to the primary and secondary zones of deformational behavior pointed out earlier by Murayama et al.[2),3)] in the series of trap door experiments. Confirming the presence of these zones is equivalent to acknowledging formation of shear bands ***a*** and ***b***, which may not be a desirable practice in view of minimizing deformation during construction of shallow tunnels. However, it is regarded very important that a reliable method be established in order to reveal non-linear deformational mechanism and identify the state of deformation with reference to an ultimate state, which is of current interest in the new design practice.

4. STRAIN SOFTENING ANALYSIS

In the framework of applying general numerical analysis tools, such as finite element methods, there have been series of approaches taken for simulation of tunnel excavation. Adachi et al.[4)] made use of classical slip line theory to define geometrical distribution of joint elements for modeling shallow tunnel excavation. Okuda et al.[5)] applied a back analysis procedure to identify the deformational mechanism, in which anisotropic damage parameter m was employed. Sterpi[7)] conducted strain softening analysis in which strength parameters (cohesion and friction angle) were lowered immediately after the initiation of plastic yielding. This approach was applied for the interpretation of field measurements by Gioda and Locatelli[8)] who succeeded to simulate the actual excavation procedure with accuracy. These attempts incorporate some of the key factors that must be taken into consideration for modeling shallow tunnel excavation. However, there still is shortage in modeling capability, which is expected to cope with development of shear bands, formation of primary and secondary zones, etc.

By reviewing the previous works, the authors concluded that the essential features to be taken into the numerical procedure would be 1) reduction of shear stiffness and 2) strength parameters after yielding (namely, strain softening)[9)]. Following is a brief summary of the procedure employed in this work. A fundamental constitutive relation between stress σ and strain ε is defined by an elasticity matrix D

$$D = \frac{E}{1-\nu-2\nu^2}\begin{bmatrix} 1-\nu & \nu & 0 \\ \nu & 1-\nu & 0 \\ 0 & 0 & m(1-\nu-2\nu^2) \end{bmatrix} \tag{1}$$

where $\sigma = D\varepsilon$ holds. E and ν stands for Young's modulus and Poisson's ratio, respectively. The anisotropy parameter m is shown in **Fig.5(a)** and defined as

$$m = m_e - (m_e - m_r)[1 - Exp\{-100\alpha(\gamma - \gamma_c)\}] \quad (2)$$

where m_e is the initial value of m, m_r is the residual value, α is a constant, γ is shear strain, γ_c is the shear strain at the onset of yielding.

The constitutive relationship is defined for conjugate slip plane direction (45° ± ϕ/2) and transformed back to the global coordinate system. Strength parameters, namely cohesion c and friction angle ϕ are reduced from the moment of initiation of yielding to residual values, as indicated in **Fig.5(b)**. This implies that the admissible space for stress is gradually shrunk as strain-softening process takes place. Any excess stress, which is computed on the transformed coordinate system based on slip plane direction, outside an updated failure envelop is converted into unbalanced forces that are compensated for in an iterative algorithm.

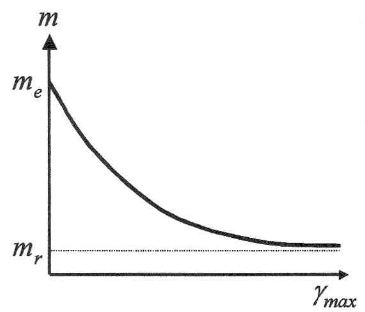

(a) Reduction of shear stiffness.

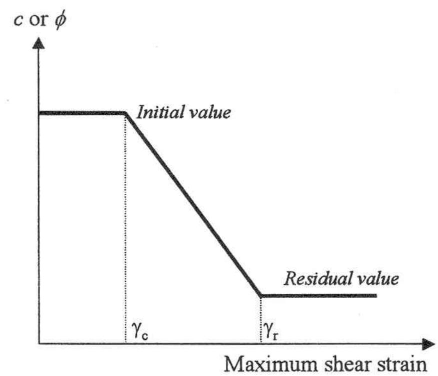

(b) Reduction of strength parameters.

Fig.5 Reduction of stiffness and strength parameters.

5. APPLICATION EXAMPLE

(1) Construction site for Rokunohe tunnel

The Rokunohe tunnel, 3810m long, is located at the northern end of the Honshu, between Hachinohe and Shin-Aomori. Two sections A and B were chosen as monitoring sections as shown in **Fig.6**. The excavation was conducted by top heading method. Excavation of the lower section excavation followed approximately 40m behind the face of the upper section excavation. Reinforcement of supports has been put by using rockbolt, shotctete and steel support as shown in **Fig.7**. Auxiliary method is applied by face shotcrete, face bolt, deep well, well point, and so on, for face stabilization and water inflow control.

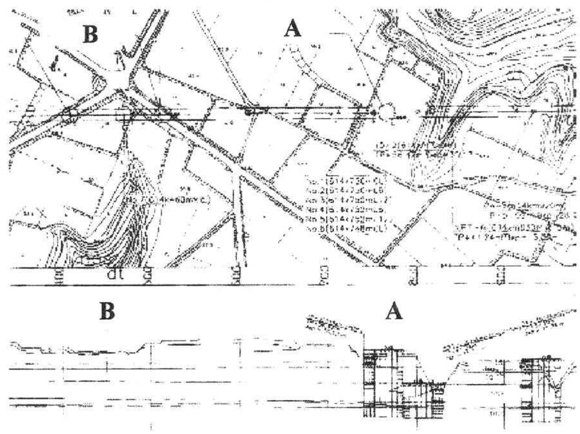

Fig.6 Plan and vertical view of the site.

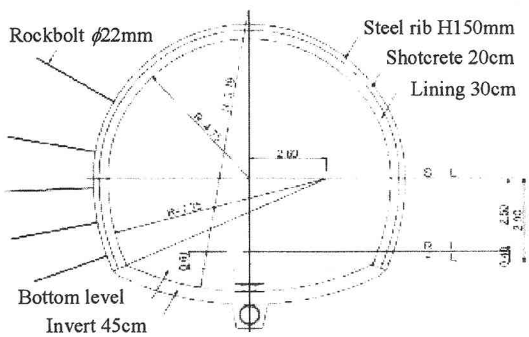

Fig.7 Tunnel cross section.

Tab.1 Material properties for 3 layers.

	Layer 1 *Takadate volcanic ash layer*	**Layer 2** *Tengutai volcanic ash layer*	**Layer 3** *Noheji sandy layer*
γ (kN/m^3)	14.0	18.0	20.0
E (MPa)	5.0	5.0	80.0
ν	0.286	0.286	0.286
ϕ (degrees)	30	45	30
c (MPa)	0	0	35

The geological profile of the ground consists of unconsolidated sand layer (Layer 3) in excess of 30m which is lying beneath two layers (Layers 1 and 2) of volcanic ash. The material properties obtained for each layer are shown in **Tab.1**. During the tunnel construction, various measurements on tunnel and ground were carried out to confirm the stability of the tunnel and the adequateness of the excavation method. Crown, convergence, surface settlement, subsurface settlement and horizontal displacement were measured as shown in **Fig.8**.

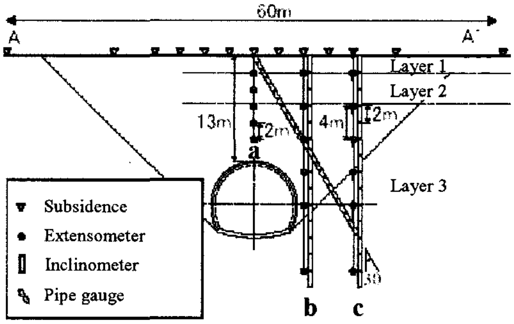

Fig.8 Field instrumentation.

(2) Outline of numerical simulation

Numerical simulations were conducted for two cross sections with slightly different geometric configuration. Locations for the two sections A and B are shown in **Fig.6**. Geometry and boundary conditions of the finite element meshes are shown in **Fig.9** for the case of Section A.

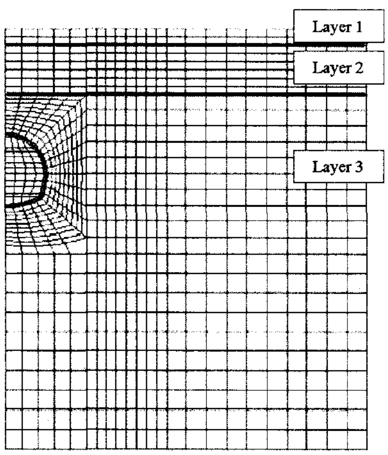

Fig.9 Finite element mesh used for simulation.

The ground behavior was modeled with three different constitutive laws; namely 1) an elastic model, 2) elastic-plastic material model with a Mohr-Coulomb failure criterion and 3) the strain softening model proposed in this paper. Shotcrete and steel support were modeled as elastic elements. The construction sequence is to excavate the top heading (upper section) in advance followed by bench (lower section) and invert excavation. Simulation has been performed in several computational steps for excavation of the tunnel top heading.

In the first step, 40% stress release ratio with excavation of the top heading (upper section) have been applied. This ratio was chosen by studying the characteristics of displacement versus time records for the cross sections of the same tunnel. This step relates to the timing when an upper section arrives at a tunnel face. In the second step, the support has been put in place and, at the same time, the remaining 60% of the excavation forces has been released.

As for strain softening analysis, parametric study was performed in which $\Delta\gamma$ (increment of maximum strain during which strength drops from peak to residual value, equal to γ_r-γ_c in **Fig.5(b)**) and the ratio of residual to initial strength were varied, resulting in the total of 9 cases as shown in **Tab.2**. In this set up, Case 1 has the least amount of parameter reduction and at the same time, the softening occurs at the slowest rate. On the other hand, Case 9 would be the severest case in which the largest reduction ratio is given at the fastest speed.

Tab.2 Scheme for strain softening analyses.

		Residual strength/Initial Strength		
		80%	60%	40%
	0.04	Case 1	Case 4	Case 7
$\Delta\gamma$	0.02	Case 2	Case 5	Case 8
	0.01	Case 3	Case 6	Case 9

(3) Subsidence profile

Fig.10 shows surface subsidence from 3 different material models and the measurement defined immediately after the completion of the tunnel invert. As for the results of strain softening analysis, the one which gave the closest results to the measurement is shown for both cross sections A and B. For section A, where the maximum subsidence was around 10mm, the results from different models show insignificant differences. On the contrary, those for section B, where the displacement in excess of 50mm was measured; the superiority of the softening model is seen as compared to elastic or elasto-plastic analysis. A clear advantage of the strain softening analysis is seen here for section B, where the shear band development might have occurred to produce this particular profile of surface subsidence. The exact reason for having such a large difference between deformations of sections A and B, is yet to be known, however, it is suspected that some differences in construction sequencing or state of underground water might have been the cause.

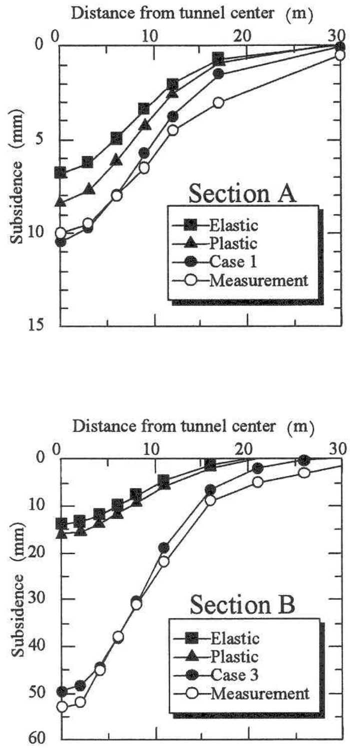

Fig.10 Surface subsidence immediately after the completion of tunnel invert.

(4) Distribution of maximum shear strain

Finally, **Fig.11** shows the maximum shear strain distribution at the final stage of analysis for sections A and B. It is seen for section A, all material models resulted in similar images since the magnitude of displacement here was constrained to fairly low level. However, for section B, the case which showed the best results in comparison with the measurement, namely the result from the softening analysis, shows the development of shear band from tunnel shoulder. The band is believed to be of a fair size, although it has not reached the surface of the ground. However, this development of the shear band is regarded as the cause of large displacement that occurred for this section.

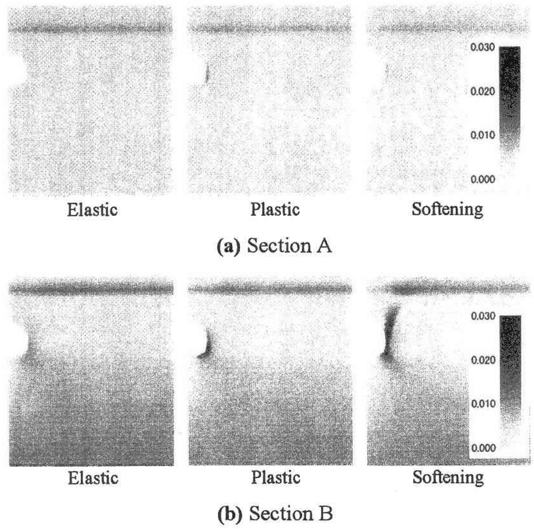

Fig.11 Maximum shear strain distribution at final stage.

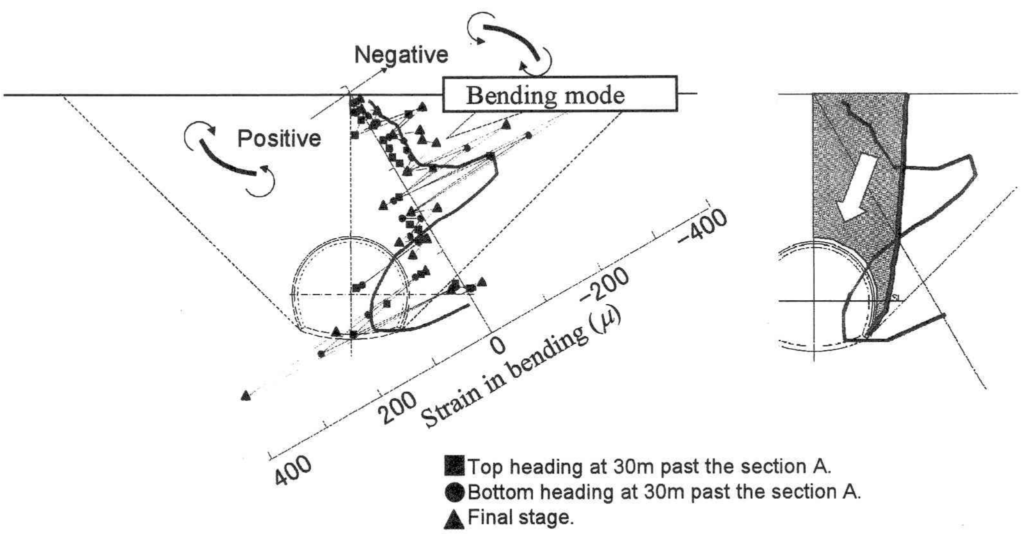

Fig.12 Bending of pipe gauge embedded in section A.

(5) Pipe gauge in section A

Whereas the strain level for section A was found to be much lower than that for section B, the reading obtained from the pipe gauge embedded in section A showed an interesting behavior shown in **Fig.12**. Though the magnitude of deformation is small, the bending mode of the pipe which was installed at an inclined position suggests that the shear band formation was already in progress to some extent. This is not an easy phenomenon to identify from standard pattern of displacement monitoring, but definitely a very important behavior not to be missed.

6. PREDICTION

(1) Principle and method for prediction

As pointed out earlier, it is ideal if deformation at final stage could be predicted before construction using lab test results and etc. However, it is well known that direct use of lab test results would not lead to realistic estimate of the final state of deformation around tunnels. As an alternative and pragmatic way of prediction, parameter identification at earlier stages of construction and use of those parameters for prediction in remaining sequences of construction is recommended.

In this study, a set of 9 cases were analyzed for each stage of construction with varying parameters. In order to perform predictive analyses, it was decided not to select only one set of so-called "*best parameters*". Instead, the first set of parameters was selected such that the use of them would produce the minimum estimate of displacement at the final stage. Likewise, the second set of parameters was selected such that they would lead to the maximum estimate of displacement. By this method, one would obtain a band of displacement values within which the real values should fall.

(2) Prediction of surface settlement

Firstly, two sets of parameters were determined from the lab test results, from which the prediction was made for the final stage for section A, which is shown in **Fig.13(a)**. As obvious the prediction made at this stage is very low in quality. **Fig13(b)** shows the results of similar exercise in which two sets of parameters were determined considering measured results at the arrival of the top heading. One would notice that the two predictions show realistic band of displacement and finds that the actual measurement lies by the maximum estimate. Fig.**13(c)** shows the similar results obtained after the completion of the top heading. The difference between the two predictions is now smaller than before and the reality lies again near the maximum estimate. **Fig.14** shows the results obtained for section B, which are well in accordance with those obtained for section A.

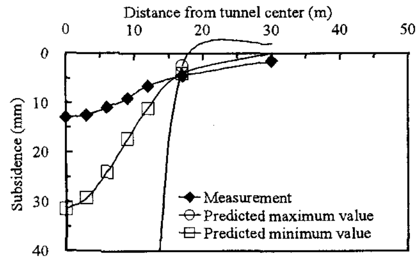

(a) Prediction using lab test results.

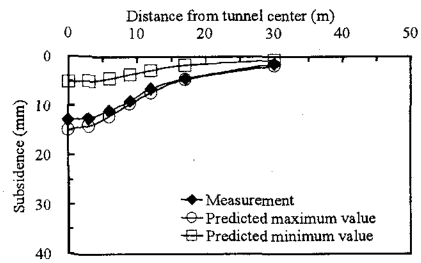

(b) Prediction made after the arrival of top heading.

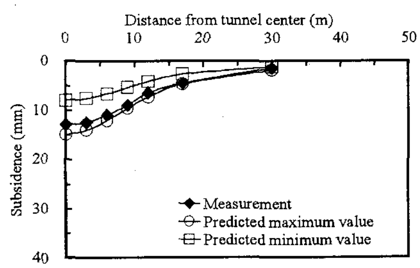

(c) Prediction made after the completion of top heading.

Fig.13 Minimum and maximum estimates of displacement at the final stage for section A.

(3) Prediction of displacement around tunnel

Since the section A was heavily monitored as shown in **Fig.8**, the similar check is performed firstly for displacement measured around the tunnel at section A. The minimum and maximum predictions made at the completion of the top heading are shown in **Fig.15** for three locations (**a**, **b**, and **c** in **Fig.8**). In this case, the actual measurement results lie closer to the minimum predictions for all three locations. **Fig.16** shows one graph illustrating the minimum and maximum predictions at line **b** for section B.

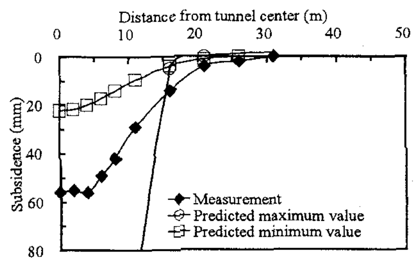

(a) Prediction using lab test results.

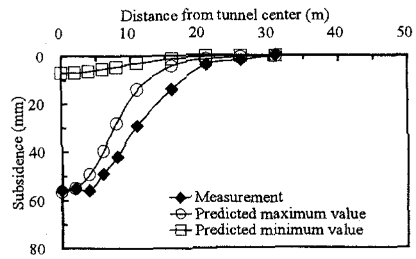

(b) Prediction made after the arrival of top heading.

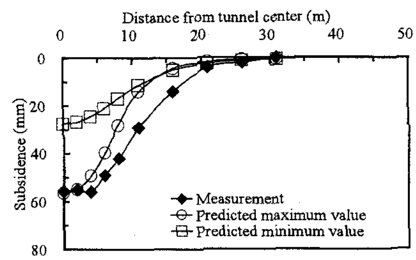

(c) Prediction made after the completion of top heading.

Fig.14 Minimum and maximum estimates of displacement at the final stage for section B.

The actual behavior fell within the band of two predictions in this case as well.

(4) Implication of predictive analyses

As shown here, the band defined between minimum and maximum predictions could be regarded as a most likely zone within which final displacements would fall. One could also take the minimum prediction as a guide line for safety assessment where a warning could be issued once the actual displacement exceeds this threshold.

It should also be noticed that the width of the band tends to decrease at later stages of construction, which is ideal from practical point of view.

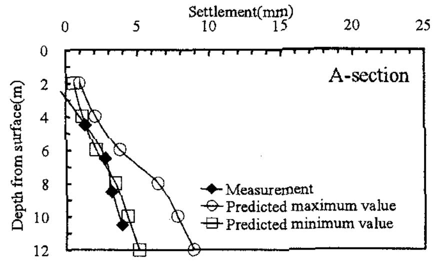

(a) Extensometer above the tunnel (line **a**).

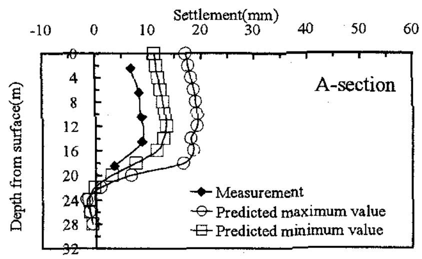

(b) Extensometer at near side (line **b**).

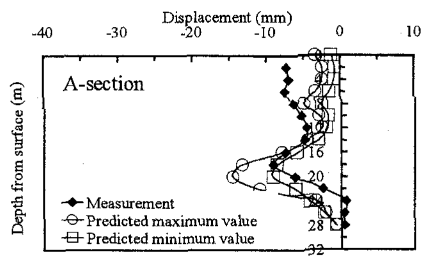

(c) Inclinometer (line **b**).

Fig.15 Minimum and maximum estimates of displacement around tunnel at the final stage for section A.

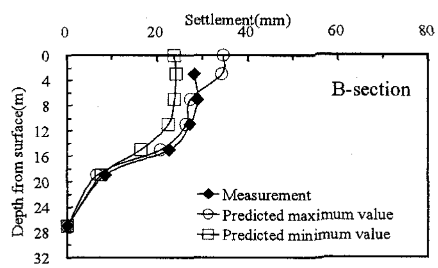

Fig.16 Minimum and maximum estimates of displacement around tunnel at the final stage for section B.

7. CONCLUSION

A non-linear finite element analysis procedure was proposed for modeling a deformational behavior, which is unique to tunnels with shallow depth. An objective was to point out the importance of modeling a non-linear nature of the deformational mechanism for obtaining a better understanding of design load on tunnel linings and its relation to kinematics of the surrounding ground. The results obtained showed that modeling of a ground behavior, which is essentially of non-linear nature, by an elastic or elastic-perfectly plastic approach, leads to incorrect understanding of the deformational mechanism. The proposed approach produced strain distribution, deformational mechanism, surface settlement profile, which were in good agreement with the results of the field measurement results for two cross sections that showed different deformational behaviors.

It was also shown that the realistic prediction of the final state of deformation could be made at relatively early stage, for example at the completion of top heading, using minimum and maximum predictions. The employment of this banded-prediction also helps engineers in safety assessment.

Use of the proposed approach would enable a better understanding of deformational characteristics of the ground medium not only in identifying local plastic zones, but also in revealing kinematics of movement of blocks formed between slip planes, or shear bands. Furthermore, the method offers a practical way for predicting final displacement of tunnel at earlier stages of construction, enabling rational safety management scheme to be employed. This makes a good starting point for optimizing ground support for reducing surface settlement, considering a particular nature of the deformational mechanism of shallow tunnels.

ACKNOWLEDGMENT: This research was conducted under the Technical Committee of Tohoku Shin-kansen Tunnel organized by the Japan Railway Construction, Transport and Technology Agency. Also, technical contributions from Mr K. Yashiro of Japan Railway Research Institute, Mr T. Sudo of Taisei Corporation, Mr N. Doba of Kajima Corporation are greatly appreciated.

REFERENCES

1) O'Reilly, M.P. and New, B. M.: Settlements above tunnels in the United Kingdom-their magnitude and prediction, *Proceedings of Tunneling 1982*, Institute of Mining Metallurgy, London, pp.73-188, 1982.
2) Murayama, S. and Matsuoka, H. : 1969. On the settlement of granular media caused by the local yielding in the media, *Proceedings of JSCE*, Vol.172, pp.31-41, 1969. *(in Japanese)*
3) Murayama, S. and Matsuoka, H. : 1971. Earth pressure on tunnels in sandy ground, *Proceedings of the JSCE*, Vol.187, pp.95-108, 1971. *(in Japanese)*
4) Adachi, T., Tamura, T. and Yashima, A. : Behavior and simulation of sandy ground tunnel, *Proceedings of the JSCE*, 358(III-3), pp.129-136, 1985. *(in Japanese)*
5) Okuda, M., Abe, T. and Sakurai, S. : Nonlinear analysis of a shallow tunnel, *Journal of Geotechnical Engineering*, JSCE, 638(III-49): pp.383-388., 1999. *(in Japanese)*
6) Hansmire, W. H. & Cording, E. J. : Soil tunnel test section : Case history summary, *Journal of Geotechnical Engineering*, ASCE, 111(11): pp.1301-1320. 1985.
7) Sterpi, D.: An analysis of geotechnical problems involving strain softening effects, *International Journal for Numerical and Analytical Methods in Geomechanics*, Vol.23, pp.1427-1454. 1999.
8) Gioda, G. & Locatelli, L. : Back analysis of the measurements performed during the excavation of a shallow tunnel in sand, *International Journal for Numerical and Analytical Methods in Geomechanics*, Vol. 23, pp.1407-1425. 1999.
9) Akutagawa, S., Kitani, T. ,Matsumoto, K. and Mizoguchi, S.: Numerical modeling of a nonlinear deformational behavior of a tunnel with shallow depth, *Modern Tunneling Science and Technology, (IS -Kyoto)*, Adachi et al eds, pp.111-114, 200 .